Modulation instability, Akhmediev breathers, and "rogue waves" in nonlinear fiber optics

J.M. Dudley, G. Genty, F. Dias, B. Kibler, N. Akhmediev

▶ **To cite this version:**

J.M. Dudley, G. Genty, F. Dias, B. Kibler, N. Akhmediev. Modulation instability, Akhmediev breathers, and "rogue waves" in nonlinear fiber optics. SPIE Laser 2010: 7th Conference on Fiber Lasers - Technology, Systems, and Applications, Jan 2010, San Fransisco, United States. pp.758029, 10.1117/12.841317 . hal-00563264

HAL Id: hal-00563264
https://hal.science/hal-00563264

Submitted on 18 Apr 2021

HAL is a multi-disciplinary open access archive for the deposit and dissemination of scientific research documents, whether they are published or not. The documents may come from teaching and research institutions in France or abroad, or from public or private research centers.

L'archive ouverte pluridisciplinaire **HAL**, est destinée au dépôt et à la diffusion de documents scientifiques de niveau recherche, publiés ou non, émanant des établissements d'enseignement et de recherche français ou étrangers, des laboratoires publics ou privés.

Distributed under a Creative Commons Attribution 4.0 International License

Modulation instability, Akhmediev breathers, and "rogue waves" in nonlinear fiber optics

John M. Dudley[a], Goëry Genty[b], Frederic Dias[c], Bertrand Kibler[d], and Nail Akhmediev[e]
[a] Université de Franche-Comté, Institut FEMTO-ST, 25030 Besançon, France
[b] Tampere University of Technology, Optics Laboratory, FI-33101 Tampere, Finland
[c] Centre de Mathématique et de Leurs Applications (CMLA), ENS Cachan, France
[d] CNRS/Université de Bourgogne, Institut Carnot de Bourgogne, 21078 Dijon, France
[e] Australian National University, Institute of Advanced Studies, Canberra ACT 0200, Australia

ABSTRACT

The development of the supercontinuum spectrum in the quasi-CW regime is studied analytically, numerically and experimentally. An interpretation in terms of localized periodic structures known as "Akhmediev Breathers" is proposed. Theory, numerical simulation and experiment are in excellent agreement. We also briefly consider the role of breather collisions in the presence of higher order dispersion and show that they lead to the formation of very large amplitude localized structures that may be analogous to the infamous oceanic rogue waves.

Keywords: Solitons, nonlinear optics, supercontinuum generation, photonic crystal fiber, rogue waves.

1. INTRODUCTION

There is currently a great deal of interest in the characteristics of extreme-value fluctuations in optical fibre supercontinuum (SC) generation [X1-3]. In particular, although many aspects of fibre SC generation are now well-understood [4,5] these recent results have shown how noise-induced fluctuations in the long pulse quasi-CW regime can modify the dynamics so as to lead to very rare cases where high amplitude "optical rogue waves" are generated. A central challenge in understanding these rare events is of course to develop rigorous models linking the complex generation dynamics and the associated statistical behavior. In this regard, although the initial description of optical rogue waves was applied to rare high amplitude soliton pulses generated on the long-wavelength edge of a broadband fibre SC spectrum, there has recently been an improved understanding that a more likely analogy with the oceanic case is to be found in the onset phase of supercontinuum generation when coherent breather structures begin to emerge [6, 7].

Significantly, it has also recently been realised that the spectral characteristics seen in this emergent SC regime can be described using powerful analytic techniques [8]. In fact, despite intensive research over three decades, there are surprisingly-few analytic solutions describing nonlinear pulse evolution in optical fibers. Certainly there are exceptions such as the well-known soliton and self-similar solutions [9], but complex processes such as supercontinuum generation have generally been considered to require numerical approaches. In this paper, however, we summarize recent results that have shown that an analytic theory of "Akhmediev Breather" (AB) propagation [10] can be successfully applied to quantitatively explain the form of the developing SC spectrum under long-pulse excitation conditions. We show that the AB theory provides new insight into the properties of the initial broadening and nonlinear spectral transformation of CW supercontinuum generation seeded by noise. We discuss how the temporal structure that develops from spontaneous modulation instability (MI) can be naturally interpreted in terms of the characteristics of AB evolution, and we show how the frequency-domain properties of the maximally-compressed AB solution reproduce the characteristic triangular shape of the MI spectrum when plotted on a semi-logarithmic scale. Numerical and analytic results are confirmed by experimental studies of quasi-CW spectral broadening induced by nanosecond pulse pumping in the anomalous dispersion regime of a photonic crystal fiber (PCF). Finally, we present simulations that go beyond the initial phase of AB evolution in the presence of symmetry-breaking third-order dispersion. We show that this leads to collisions and interactions between the emergent localized AB structures that may provide a natural link to the instabilities that occur in an oceanographic context.

2. THEORETICAL SUMMARY

The AB theory we present here was developed in mid-1980s by Akhmediev and co-workers who used an insightful analytical approach to construct novel solutions to the nonlinear Schrodinger equation describing fiber propagation. We first write the NLSE in dimensional form [4]:

$$i\frac{\partial A}{\partial z}+\frac{\beta_2}{2}\frac{\partial^2 A}{\partial T^2}+\gamma|A|^2 A=0\,, \tag{1}$$

where $|A|^2$ has dimensions of instantaneous power in W and the dispersion and nonlinearity coefficients β_2 (< 0) and γ have dimensions of $ps^2\ km^{-1}$ and $W^{-1}\ km^{-1}$ respectively. The AB solution describes the evolution along z of a wave with initial constant amplitude on which is superimposed a small periodic perturbation taking the form of a T-dependent low amplitude modulation. The solution then consists of an evolving train of ultrashort pulses that is periodic in T and that exhibits a recurrence (growth-return) cycle in z.

In contrast to soliton solutions which are localized in T, the ideal breather solution is localised in the z direction. In fact, certain initial conditions can also yield periodic evolution along the z-direction, but even in this case, the pulse train characteristics nonetheless remain well-described by the analytic AB solution. The AB solution to Eq. (1) is :

$$A(z,T)=\sqrt{P_0}\ \frac{(1-4a)\cosh(bz)+ib\sinh(bz)+\sqrt{2a}\cos(\omega_{\mathrm{mod}}T)}{\sqrt{2a}\cos(\omega_{\mathrm{mod}}T)-\cosh(bz)}, \tag{2}$$

which shows growth-return evolution over $-\infty < z < \infty$. The variable independent parameter ω_{mod} is the (perturbation) frequency of the initial temporal modulation. Coefficients a and b depend on ω_{mod}, defined by: $2a = [1 - (\omega_{\mathrm{mod}}/\omega_c)^2]$ and $b = [8a\,(1\text{-}2a)]^{1/2}$ with $\omega_c^2 = 4\gamma P_0/|\beta_2|$ and P_0 the CW power at large $|z|$. The solution is valid over modulation frequencies that experience MI gain: $\omega_c > \omega_{\mathrm{mod}} > 0$ such that a varies in the interval $0 < a < 1/2$ while the parameter $b > 0$ governs the MI growth. Maximum gain $b = 1$ occurs for $a = 1/4$, i.e. $\omega_{\mathrm{mod}} = \omega_c/\sqrt{2}$. The solution in Eq. (2) describes an evolving periodic train of ultrashort pulses with temporal period $T_{\mathrm{mod}} = 2\pi/\omega_{\mathrm{mod}}$. The individual temporal sub-pulses have maximum amplitude and minimum temporal width at $z = 0$. The solution here describes the "maximally-compressed" AB :

$$A(z=0,T)=\sqrt{P_0}\ \frac{(1-4a)+\sqrt{2a}\cos(\omega_{\mathrm{mod}}T)}{\sqrt{2a}\cos(\omega_{\mathrm{mod}}T)-1}. \tag{3}$$

The corresponding spectrum consists of discrete frequency sideband modes with separation ω_{mod}, and intensities that decrease following a geometric progression. For the particular case of the maximally-compressed solution of Eq. (3), the mode intensities are: $S_0 = P_0\,(2^{1/2}\text{-}1)^2$ for the pump, and $S_n = 2\,P_0\,(2^{1/2}\text{-}1)^{2|n|}$ (where $n = \pm1, \pm2, \pm3, \ldots$) for the sidebands. Thus the pump and sideband intensities follow the relative progression $\{I_0, I_1, I_2, I_3, I_4\ldots\} = \{1, 2, 0.3431, 0.0589, 0.0101\ldots\}$ so that there is a 3 dB increase from the pump (n=0) to the first sideband (n=±1) and then a constant decrease of $20\ \log_{10}(2^{1/2}\text{-}1) = -7.66$ dB between subsequent sidebands. This geometric progression yields a characteristic triangular shape in the wings of the spectrum when plotted semi-logarithmically.

3. EXPERIMENTAL RESULTS FOR SUPERCONTINUUM GENERATION

We now present some experimental results: Fig. 1(a) shows spectral measurements at the output of 3.9 m of a highly nonlinear photonic crystal fiber with zero-dispersion wavelength at 780 nm for various peak powers using 1 ns pulses from a passively-modelocked microchip laser operating at 1064 nm. The experiment results in the top panel are compared with generalised nonlinear Schrödinger equation (GNLSE) simulations in the bottom panels. Full simulation details are to be found in Ref. [10] but we note that the major parameters were: $\beta_2 = -75\ ps^2\ km^{-1}$ and $\gamma = 60\ W^{-1}\ km^{-1}$. We note immediately that the agreement between experiment and simulation is very good and illustrate the key steps of initial sideband development followed by the merging and formation of a continuous triangular pedestal about the pump. At the lowest power of 26 W, the spectrum consists of small number of distinct sidebands separated by the frequency of peak MI gain. As the power increases to 43 W, we enter an "extended MI" regime where we can still resolve sidebands close to the pump, but we also see the development of continuous low amplitude wings that appear triangular when plotted with a semi-logarithmic y-axis. The spectral width in this regime approaches 60 nm at the -40 dB level, and we note the first sign of a very low amplitude Raman peak around 1120 nm. At higher power levels (not shown), the characteristics of a "fully-developed" supercontinuum are observed [5].

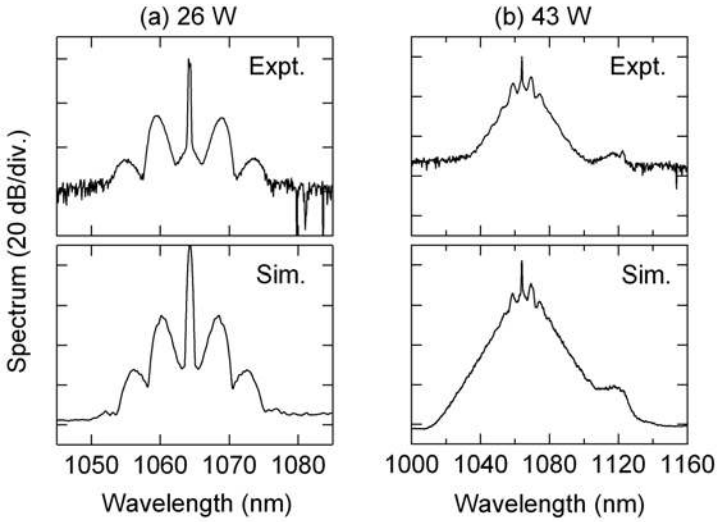

Fig. 1. Experimental results (top) and simulation results (bottom) results at peak powers as shown (see text).

We focus particular attention on the characteristics of the extended MI spectrum at 43 W peak power. In fact, although we have used GNLSE simulations in Fig. 1(b), this power level actually describes a regime before the onset of higher-order effects become significant and we might expect the AB theory to provide a good description. To examine how the AB theory can be applied to interpret the properties of the broadened spectrum seen at 43 W, Fig. 2 shows in more detail how the temporal properties associated with the extended MI phase develop with distance.

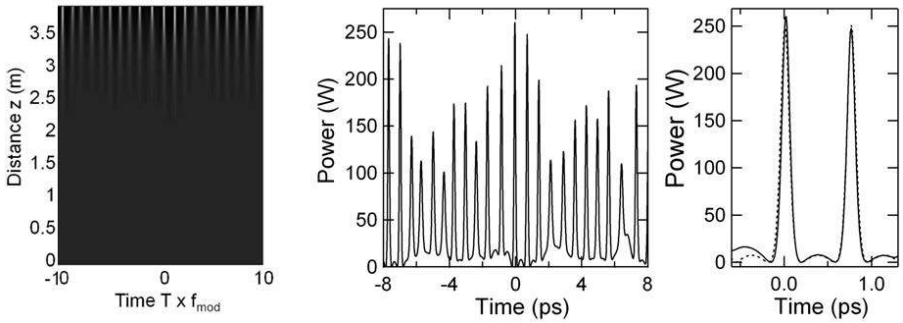

Fig. 2. Single shot temporal evolution. A detail of the extracted temporal trace is shown in the rightmost figure, comparing simulations (solid line) with the AB solution at a modulation frequency corresponding to peak MI gain (dashed line).

The simulations use fiber parameters corresponding to experiment, and assume 43 W peak power CW field with noise. The grayscale plot shows a single numerical realization illustrating temporal evolution over 3.9 m. At a distance of 3.5 m we extract the temporal profile that shows a high contrast pulse train, but the broadband noise that seeds the MI results in significant variation in the structure of the individual temporal peaks. Nonetheless, the highest amplitude peaks in the temporal profile (shown in the detailed view) are fitted very well by the maximally-compressed AB sub-pulses calculated from Eq. (3) using ω_{mod} corresponding to the peak of the MI gain (f_{mod} = 1.32 THz for our parameters.) In fact, analysis of the highest-amplitude peaks at other regions of the profile (not shown) reveals similarly good agreement with the calculated AB solution, and we have confirmed that simulations using different noise seeds reveal the same characteristics.

These results suggest that the extended MI spectrum in Fig. 1(b) in fact contains a dominant contribution from spontaneously-generated AB sub-pulses generated at the peak of the MI gain. Indeed, we can confirm this using experimental spectral measurement by comparing the form of the measured spectrum with the geometric progression predicted for the maximally-compressed AB. Figure 3 compares numerical and analytic results with the experimental results of Fig. 1 for P_0 = 43 W. Specifically, the numerical results show averaged multi-shot simulations using the full GNLSE with a 1 ns pulse input field (blue, short dashes) and using only the NLSE with a CW input field

(red, long dashes). It is clear that both GNLSE and NLSE simulations produce similar results in agreement with experiment, with the GNLSE of course also predicting the onset of a small Raman peak on the long wavelength edge around 1120 nm; but this is largely insignificant in the context of the conclusions drawn here relating to AB dynamics.

A significant result here is excellent agreement between the experimental decay of the spectral wings and the calculated amplitudes of the discrete frequency modes associated with the analytic form of the maximally-compressed AB. Because spontaneous MI is seeded by broadband noise, the spectral structure is of course not discrete, but rather consists of a continuous span of frequencies. Nonetheless, as with the time domain characteristics, we expect the spectral characteristics to contain a dominant component from the maximally-compressed AB solution calculated at peak MI gain. Thus, normalising to the $n = \pm 1$ sideband amplitudes of experiment, the decay of spectral intensity with frequency in experiment and simulations is reproduced very well by the analytic geometric progression of the maximally-compressed AB breather.

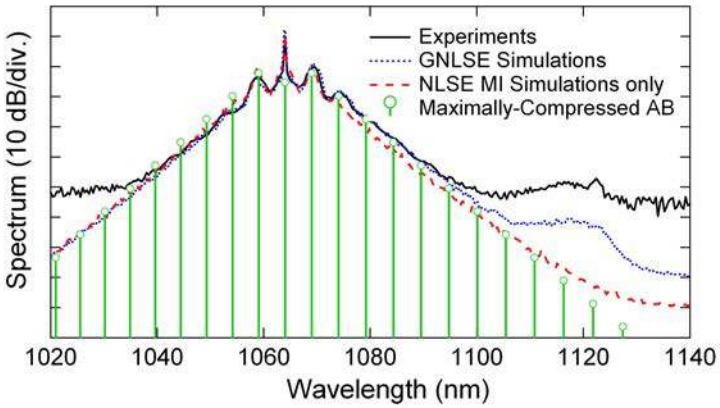

Fig. 3 Experiments (black line),simulations using the full GNLSE (blue dashed line), numerical simulations using the NLSE only (red dashed line), and the calculated spectrum of the maximally-compressed AB (green lines from zero).

4. BEYOND BREATHERS

These results have shown that the characteristics of both the modulated temporal profile and the associated spectrum in emergent SC generation can be explained in terms of the development of high amplitude Akhmediev Breather sub-pulses. This interpretation represents an important step in applying the formalism of breather evolution to the interpretation of supercontinuum generation. But of course this is not a complete explanation of how these sub-pulses subsequently separate from the extended MI spectrum and temporal pulse train and evolve towards higher-amplitude pulses that exhibit rogue wave statistics. In this context, however we note that the extended MI regime where the AB theory works well is essentially described by the integrable NLSE with noise, but any realistic optical fiber system would contain symmetry-breaking physical effects due to odd orders of chromatic dispersion and Raman scattering. In fact, both these effects are important in that they can induce collisions between the emergent breathers, but for illustrative purposes, we consider only the effect of third order dispersion in the results that follow.

In particular, Fig. 4 shows results where we have included the effect of third-order dispersion (TOD) in our simulations and we can see how it modifies the AB dynamics after the initial MI phase. These simulations use parameters different to those described above with a zero dispersion wavelength much closer to the pump. Specifically, we model 100 W, 5 ps FWHM Gaussian pulses at 1060 nm propagating in 20 m of photonic crystal fiber with zero dispersion at 1040 nm. dispersion coefficients at the pump wavelength are: $\beta_2 = -4.10 \times 10^{-1}$ ps^2 km^{-1}, $\beta_3 = 6.87 \times 10^{-2}$ ps^3 km^{-1}and the nonlinearity parameter is: $\gamma = 0.011$ W^{-1} m^{-1}. The input pulse soliton number for these parameters is $N \sim 147$, and we see clearly from Fig. 4 how the dynamics are clearly in the long pulse regime. This figure shows a detailed view of the evolution over a portion of the temporal pulse envelope, and we see the clear development of a high contrast modulation as in Fig. 2. However, the modulation is not stationary relative to the reference frame of the pump group velocity, but rather drifts towards larger co-moving time ie: towards the pulse trailing edge. This is a consequence of the TOD. In fact, we see that the combination of the TOD and noise for this case actually results in a non-uniformity in the drift behavior such that collisions can occur between different regions of the modulated field. As a result of these collisions,

we see large amplitude localization and the emergence of precursor soliton structures with peak powers ~800 W in comparison with the 200 W peak powers seen for the breathers.

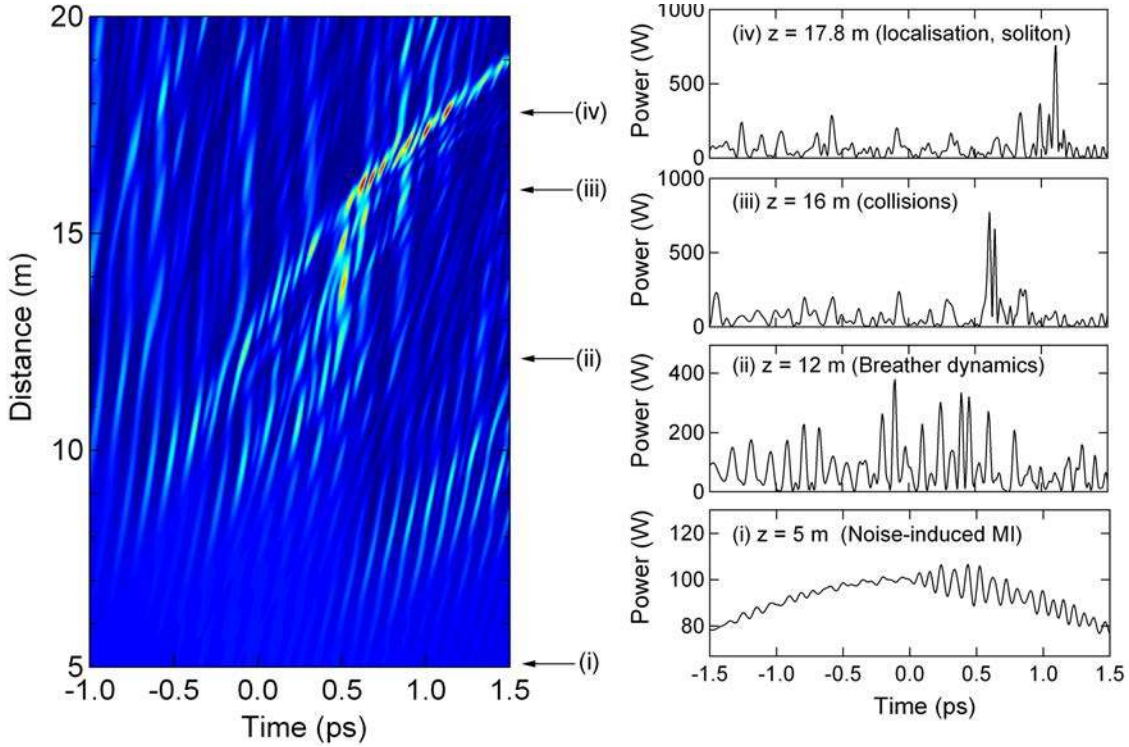

Fig. 4 Detailed view of propagation in the NLSE with noise and TOD. Initially, noise-induced MI generates high-contrast AB-like pulses, but the effect of dispersion induces an additional phase of interactions, collisions and localisation.

5. CONCLUSIONS

There are several main conclusions to make based on the results above. Firstly, numerical studies of the temporal and spectral properties of spontaneous MI have shown that the characteristics of both the modulated temporal profile and the associated spectrum can be explained in terms of the development of high amplitude AB sub-pulses. The well-known triangular form of the spontaneous MI spectrum when plotted semi-logarithmically has been explained naturally in terms of the analytic geometric progression describing the frequency dependence of the AB modal amplitudes. The analytic form of the AB spectrum has also been shown to be in very good quantitative agreement with the wings of the spontaneous MI spectrum observed in experiments studying the onset of quasi-CW supercontinuum generation. In addition, other results have shown that SC generation described by an NLSE model perturbed only by TOD can lead to large amplitude localized optical rogue soliton and rogue wave structures. Generally speaking, any single perturbation that destroys the integrability of the NLSE is sufficient to observe "survival of the fittest" soliton amplification as a result of collisions. Our simulations also yield the qualitative observation that collisions between emerging breather structures from an envelope undergoing MI appears to be a precursor to the formation of rogue soliton pulses, and it is possible to conjecture that a difference in relative velocities between breathers formed across an initial wave field is an important (perhaps necessary) condition for rogue soliton emergence. In fact, although the rogue solitons in fibre optics separate distinctly from the initial field because of self-frequency shifting, it is likely that the emergent and colliding breather structures provide a closer analogy with nonlinearity-induced rogue waves on the ocean. This proposal may have wide impact, as it implies that the seeds of rogue wave formation in optics as well as hydrodynamics may be found by identifying particular wave field characteristics (initial conditions, noise frequency content or topography that favor significant breather velocity gradients.

REFERENCES

[1] D. R. Solli et al. "Optical rogue waves," Nature **450**, 1054-1057 (2007)

[2] J. M. Dudley, G. Genty, B. J. Eggleton, "Harnessing and control of optical rogue waves in supercontinuum generation," Opt. Express **16**, 3644-3651 (2008)

[3] M. Erkintalo, G. Genty, and J. M. Dudley, "Rogue wave like characteristics in femtosecond supercontinuum generation," Opt. Lett. **34**, 2468-2470 (2009)

[4] G. P. Agrawal, *Nonlinear Fiber Optics*. 4th Edition. Academic Press, Boston (2007)

[5] J. M. Dudley, G. Genty, and S. Coen, "Supercontinuum Generation in Photonic Crystal Fiber", Rev. Mod. Phys. **78,** 1135-1184 (2006).

[6] N. Akhmediev, A. Ankiewicz, M. Taki, "Waves that appear from nowhere and disappear without a trace," Phys. Lett. A **373**, 675-678 (2009)

[7] N. Akhmediev, J. M. Soto-Crespo, A. Ankiewicz, "Extreme waves that appear from nowhere: On the nature of rogue waves," Phys. Lett. A **373**, 2137-2145 (2009)

[8] 10 N. Akhmediev and V. I. Korneev, "Modulation instability and periodic solutions of the nonlinear Schrodinger equation," Theor. Math. Phys. **69**, 1089-1093 (1986)

[9] J. M. Dudley, C. Finot, D. J. Richardson, G, Millot, "Self Similarity in Ultrafast Nonlinear Optics", Nature Physics **3** 597-603 (2007).

[10] J. M. Dudley, G. Genty, F. Dias, B. Kibler, N. Akhmediev, "Modulation instability, Akhmediev Breathers and continuous wave supercontinuum generation," Opt. Express **17,** 21497-21508 (2009)